Numerical Simulation of Impact Response for Gas Turbine Support Legs

Yingdong Dai, Pengwei Lv*, Heng Ma, Hao Yin, Yunjie Fu, Haoyu Wang, Luyan Chen, Renyuan Liu

School of Naval Architecture and Port Engineering, Shandong Jiaotong University, Weihai, Shandong, China

**Corresponding Author*

Abstract: In order to study the dynamic response characteristics of the gas turbine legs under underwater explosion impact loads, this paper takes a certain type of gas turbine as the research object and establishes an equivalent finite element model. According to the German BV043/85 standard, the designed impact spectrum is converted into a combined triangular wave acceleration time history curve, and vertical impact condition simulation calculations are carried out. The study shows that the impact load is transmitted from the base, the impact platform to the base and then to the legs. The stress concentration occurs at the bottom of the legs and the bolt connection of the casing; the high-frequency components of the acceleration decay as it is transmitted upward along the legs; the impact response of the rear leg and the proportion of high-frequency energy are higher than those of the front leg. The research results can provide theoretical references for the research on the resistance to impact of gas turbines.

Keywords: Gas Turbine; Support Leg; Finite Element; Response Characteristics

1. Introduction

Gas turbines have become the preferred main propulsion power device for modern surface ships and military ships due to their high power, fast startup speed, and high reliability [1]. Their impact resistance is directly related to the safety and stability of the entire ship power system. Therefore, as the core component of the ship, the gas turbine must have excellent impact resistance. Normally, gas turbines are fixed to the hull base by several specially designed legs, which are the key structures to withstand and transmit impact loads [2]. In addition, the support legs also play a role in isolating and attenuating impact energy and protecting internal precision rotor blades, bearings and other core components. Its dynamic response characteristics play a decisive role in the impact resistance of the entire ship power plant. Therefore, the analysis of the impact response of gas turbine support legs is a crucial and extremely challenging topic in the field of research on ship impact resistance.

Domestic and foreign scholars have conducted extensive research on equipment impact resistance. Overseas naval countries, mainly European countries and the United States, have established a complete technical system covering the design, analysis and experimental verification of the impact resistance performance of shipborne equipment. Countries such as Germany and the United States have formulated strict impact resistance standards, such as the BV043/85 standard of Germany and the MIL-S-901D standard of the United States. This study adopts the German standard as the impact resistance standard because the BV043/85 standard provides clear time-domain load conversion formulas, and these standards are widely applied in the assessment of ship equipment [3]. In China, as the modernization of naval equipment continues to advance, impact resistance research on key equipment such as gas turbines has received increasing attention. Many domestic scientific research institutes and universities have used numerical simulation technology to carry out impact resistance analysis on equipment and plate structures of various types of ships, and have completed a large amount of exploratory work with reference to advanced foreign standards [4]. However, further in-depth research on the numerical simulation of the impact response and system performance evaluation of the gas turbine as a whole, especially its key support structures, under standard impact loads is still needed.

This article focuses on the impact response of the four outrigger structures of a certain type of gas

 Copyright @ STEMM Institute Press

turbine and uses numerical simulation methods to conduct research. First, through ABAQUS software, a finite element model including the main body of the gas turbine (simplified into a rigid mass block) and the detailed support leg structure was established to ensure that the model can accurately reflect the structural characteristics of the support legs. Secondly, the German military standard BV043/85[5] is used as the impact resistance assessment standard, and the typical impact spectrum is converted into equivalent positive and negative triangle wave history curves as input loads for calculation, and the dynamic response process of the four outriggers under the vertical impact load is obtained. Finally, all analysis results are combined to evaluate the impact resistance of the outrigger, and the response rules of the top and bottom of the outrigger are obtained.

2. Calculation Model

2.1 Establish Finite Element Model

This paper mainly studies the influence of impact loads in the rigid installation mode on the impact response characteristics of the gas turbine legs. To ensure the calculation accuracy while improving the calculation efficiency, the gas turbine model is reasonably simplified without affecting the overall structural characteristics and the distribution characteristics of the impact response. The complex internal structures such as the rotor casing are simplified as equivalent mass blocks loaded at corresponding positions, and the bolt holes in each component are ignored. The installation base and leg structure of the gas turbine are finely modeled, and the connections between components adopt binding constraints. A finite element model of the overall structure of the gas turbine is constructed.

When meshing the gas turbine, for complex parts such as the legs and key component connections, the minimum mesh size is used. For simple structures, a larger mesh size is selected to ensure the mesh quality and appropriately increase the mesh size to improve the calculation efficiency. The finite element model of the gas turbine and the meshing are shown in Figure 1.

In terms of material properties, the main structure of the gas turbine adopts ordinary structural steel, with a material density of 7900 kg/m³, an elastic modulus of 210 GPa, a yield strength of 250 MPa, and a Poisson's ratio of 0.3. The leg structure uses Ti6Al4V titanium alloy, with a density of 4430 kg/m³, an elastic modulus of 114 GPa, a yield strength of up to 930 MPa, and a Poisson's ratio of 0.34. Titanium alloy has advantages such as high specific strength, corrosion resistance, and good impact performance, and is commonly used as the material for the gas turbine legs.

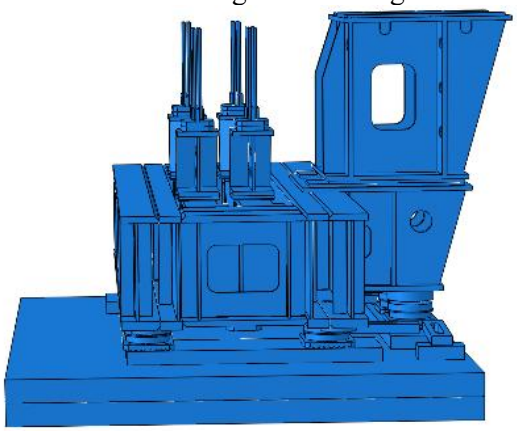

(a) Modeling of Gas Turbine Support Legs and Base Parts

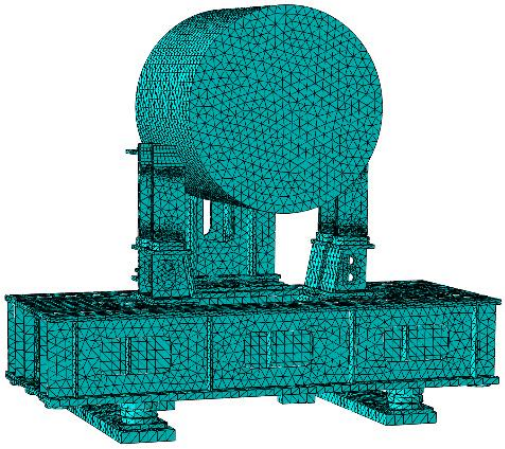

(b) Overall Mesh Division of Gas Turbine

Figure 1. Finite Element Model of Gas Turbine

2.2 Calculate Impact Load

2.2.1 Design shock response spectrum

At present, there are three typical technical routes that can be used for the assessment of impact resistance performance: the static equivalent method, the dynamic design analysis method (DDAM), and time-domain numerical simulation [6]. In this study, the time-domain simulation method was adopted, and the most stringent impact excitation input conditions specified in the German military standard BV043/85 were used to evaluate the dynamic performance of the gas turbine support legs. When the mass of shipboard equipment is less than 5 tons, some of the impact environment data specified in the German military standards are shown in Table 1.

Copyright @ STEMM Institute Press

Table 1. Part of the Impact Environment Data (Shock Spectrum) in BV043/85

Installation location	Direction	Spectral Displacement (D_0/cm)	Spectral Velocity (V_0/m·s^{-1})	Spectral Acceleration (A_0/g)
Class I	Vertical	4.3	7.0	320
	Crosswise	3.0	6.0	280
Class II	Vertical	4.2	6.0	170
	Crosswise	3.0	3.1	100
Class III	Vertical	5.2	5.0	100
	Crosswise	4.7	3.0	30

Note*: Longitudinal impact environment = Horizontal impact environment

Note**: Category I installation locations refer to the ship's outer plating or outer plating stiffeners, double bottom roof plates, and bulkheads below the main deck; Category II installation locations refer to the lower deck and the main deck, bulkheads below the main deck, and bulkheads above the main deck; Category III installation locations refer to the decks above the main deck, side bulkheads above the main deck, and middle bulkheads [7].

The German military standard BV043/85 points out that when the input excitation time history is not specified, the positive and negative triangle waves or positive and negative half-sine wave loads described below can be used for verification calculations [8]. The mass of the gas turbine model designed this time is 3.63t, which meets the impact resistance standard of less than 5t. It can be concluded from the table that the gas turbine belongs to a Category I installation location, so the impact resistance of the support legs should be checked and calculated based on the Category I vertical impact resistance standards in the specification. If the impact signal is represented in the frequency domain, the impact spectrum can be designed as shown in Figure 2.

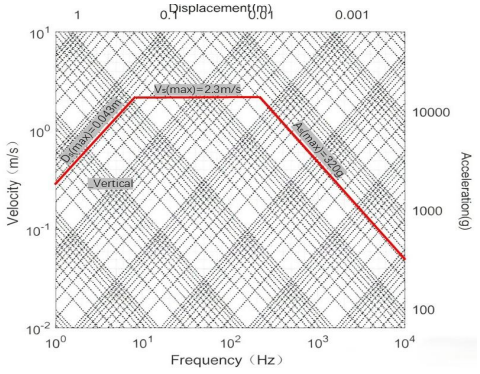

Figure 2. Typical Design Shock Spectrum

The standard design impact spectrum consists of three regions: spectral displacement, spectral velocity, and spectral acceleration regions. From the three curves, it can be seen that the two inflection points from left to right divide the entire frequency domain into three parts. The low-frequency range below the first inflection point represents spectral displacement; the middle frequency band between the two inflection points represents spectral velocity; and the high-frequency range after the second inflection point represents spectral acceleration [9]. This spectral description method can be used to quantify the impact environment caused by underwater explosions, and can be further converted into a time-domain excitation signal for the structural strength assessment of shipborne equipment.

2.2.2 Calculate impact load input

According to the BV043/85 standard, the designed spectrum is represented in the time domain as an acceleration curve consisting of a positive triangular pulse and a negative triangular pulse (Figure 3). The x-axis represents time t (seconds), and the y-axis represents acceleration a (m/s²). The peak of the positive pulse is at a_2, and the area enclosed by it is V_2; the peak of the negative pulse is at a_4. Since the areas of the two regions are equal, the final velocity of this pulse is 0 m/s². The time coordinate is defined as follows: t_2 represents the peak of the positive pulse, t_3 represents the end of the positive pulse, t_4 represents the peak value of the negative pulse, t_5 represents the end of the negative pulse. Therefore, the width of the positive pulse is $0 - t_3$, and the width of the negative pulse is $t_3 - t_5$. [10].

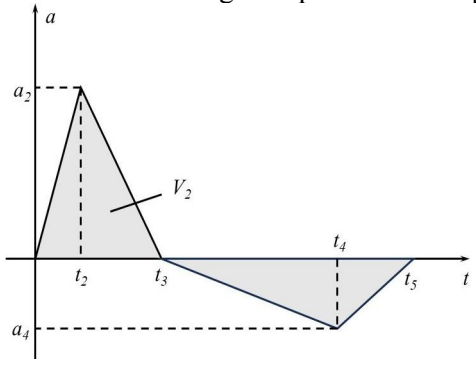

Figure 3. Combined Triangle Wave

Based on the above relationship, calculation is

 Copyright @ STEMM Institute Press

performed according to Equation (1), and the shock spectrum is converted into a time-domain acceleration positive and negative combined triangular wave history curve.

$$a_2 = 0.6 \times a_0$$

$$v_2 = \frac{3}{4} \times v_0$$

$$t_3 = 2 \times \frac{v_2}{a_2}$$

$$t_2 = 0.4 \times t_3$$

$$(t_5 - t_3) = \frac{6 \times d_0 \times 1.05 - 1.6 \times a_2 \times t_3^2}{1.6 \times a_2 \times t_3}$$

$$a_4 = \frac{-a_2 \times t_3}{t_5 - t_3}$$

$$t_4 = t_3 + 0.6(t_5 - t_3) \quad (1)$$

The parameters of each node in the combined triangle wave calculated by the above formula are shown in Table 2.

Table 2. Combined Triangle Wave Time History Curve

Parameter (Units)	Vertical
a_2/(m/s^2)	1881.6
a_4/(m/s^2)	-995.5
t_2/(s)	0.0022324
t_3/(s)	0.005581
t_4/(s)	0.0119074
t_5/(s)	0.016125

3. Response Results and Analysis

3.1 Dynamic Response Process

The model has four support legs, and typical areas and specific nodes are selected for each support leg for assessment. The location of the measuring points is shown in Figure 4.

Under the vertical impact load, the stress response cloud diagrams of the four legs at t=4ms, 8ms, 36ms, and 52ms were recorded, as shown in Figure 5.

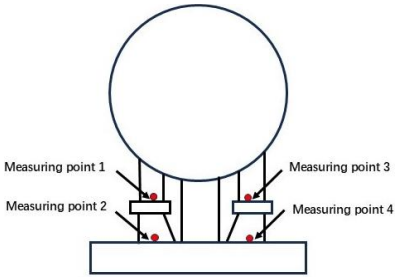

(a) Distribution of Measuring Points on the Front Outriggers

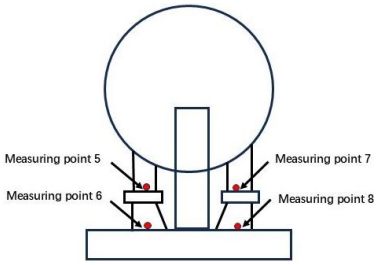

(b) Measuring Point Distribution of Rear Outriggers

Figure 4. Measuring Point Location Distribution Map

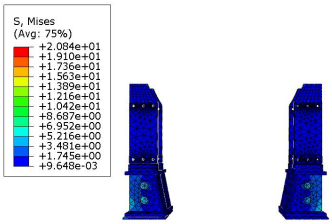

(a) t=4ms

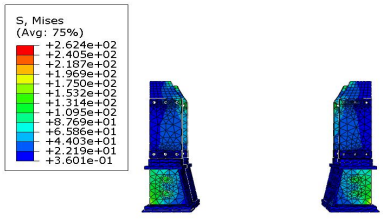

(b) t=8ms

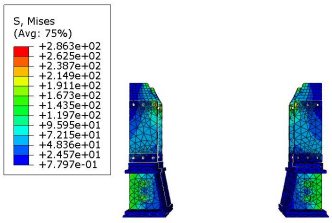

(c) t=36ms

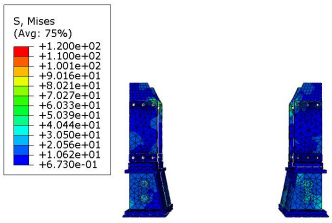

(d) t=52ms

Figure 5. Stress Response Distribution of Supporting Legs at Different Times

Figure 5 shows the stress transfer and distribution characteristics of the support legs under vertical impact load as follows: from 4ms to 8ms, the stress is concentrated at the bottom of the support leg, and there is a slight stress concentration at the connection between the upper part and the casing; from 8ms to 36ms, the stress continues to increase, and the stress concentration areas at the bottom

and the upper part become more significant; from 36ms to 52ms, the stress gradually decreases and energy dissipates. It can be seen that the stress is mainly concentrated at the structural connection points and edge areas of the support legs, among which the bolt connection between the upper part and the casing has the most obvious stress concentration, reaching 286 MPa. Although this value does not exceed the static yield limit of the material, these areas are the weak links in the anti-shock design and need to be given special attention in protection.

According to the measuring point distribution diagram in Figure 4, measuring point 1 to measuring point 8 are recorded as A1 to A8 respectively, and the acceleration curve of the representative measuring point of each leg is obtained, as shown in Figure 6.

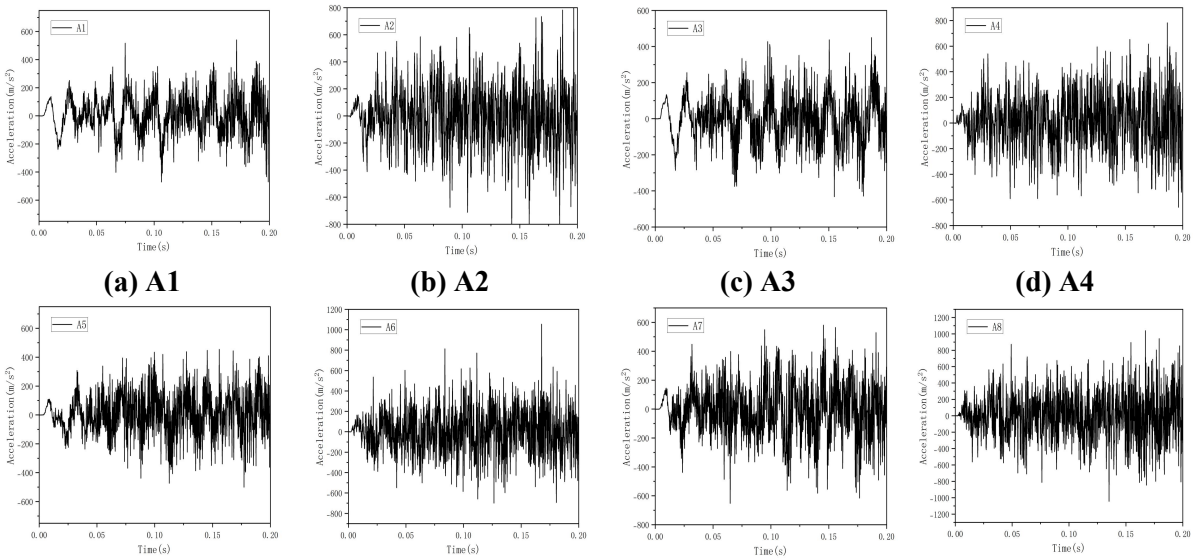

(a) A1 **(b) A2** **(c) A3** **(d) A4**

(e) A5 **(f) A6** **(g) A7** **(h) A8**

Figure 6. Acceleration Curves of Different Measuring Points

Under rigid installation conditions, there are obvious high-frequency components in the acceleration time domain. Points A1, A3, A5, and A7 are located in the upper part of the four legs; points A2, A4, A6, and A8 are located in the lower part. For the same leg, the high-frequency components in the lower part dominate, while the low-frequency components are not obvious; conversely, for the upper part of the same leg: the low-frequency components are significantly enhanced, while the high-frequency components are significantly reduced relative to the lower part points. Comparing the same horizontal position of different legs, it can be seen that the amplitude of the lower part points of the rear leg is greater than that of the front leg, and the vibration frequency density of the upper part points of the rear leg is also higher. Therefore, the acceleration response at the bottom of the leg is relatively intense, with large amplitude and high frequency. When the energy is transferred to the upper end, the high-frequency components decrease, the low-frequency components increase, and both frequency and amplitude show an overall downward trend. Throughout the process, the response of the rear leg is stronger than that of the front leg, indicating that the dynamic environment under the impact load is more intense for the rear leg.

3.2 Draw Shock Spectrum

Integrate the above-collected acceleration curves at different measuring point locations, use MATLAB mathematical modeling software to design and calculate the corresponding shock spectrum, and draw the three-fold line of the shock spectrum as shown in Figure 7.

As can be seen in the figure, there is no obvious pattern between the spectral displacement in the low-frequency band and the spectral velocity in the mid-frequency band. However, the spectral acceleration in the high-frequency band shows significant differences: the values in figures (a), (c), (e), and (g) are significantly smaller than those in figures (b), (d), (f), and (h). This indicates that the impact response in the lower part of the leg is more significant. When the impact load is transmitted from the bottom to the top of the leg, the proportion of high-frequency energy gradually decreases, and the total energy decreases synchronously with the increase in transmission distance. This phenomenon may be

 Copyright @ STEMM Institute Press

related to the flexible support structure in the leg, and it is consistent with the dispersion characteristics of the waveguide structure in the Timoshenko beam theory[11]: the low-frequency response has a longer wavelength and a faster propagation speed, and it reaches the far end of the structure first; the high-frequency response has a shorter wavelength, a slower propagation speed, and a faster energy attenuation, and it is difficult to reach a farther location.

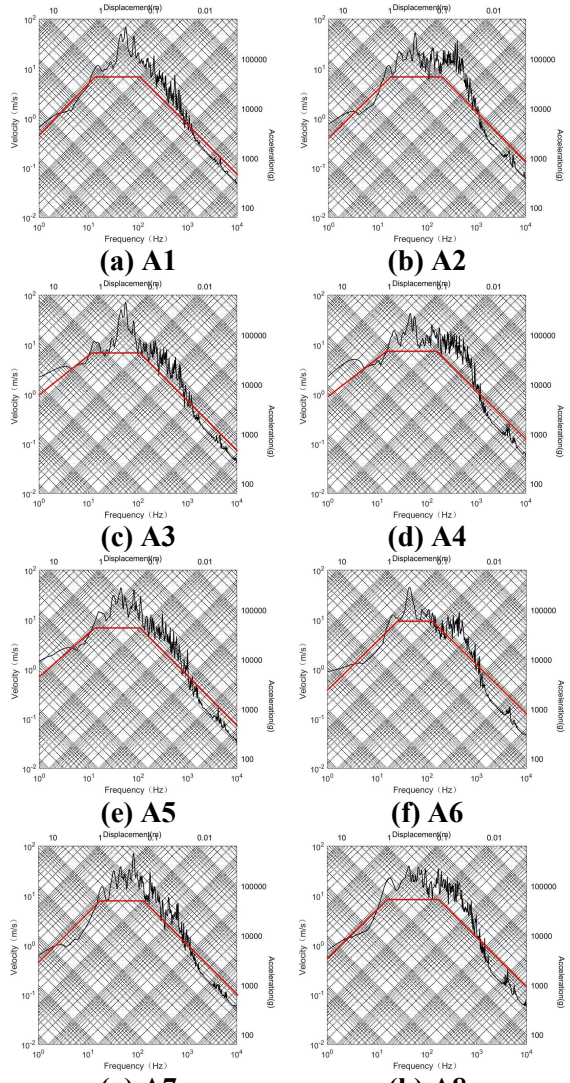

Figure 7. Three-fold Line of Impact Spectrum at Different Measuring Points

4. Conclusion

This paper conducts a numerical simulation of the gas turbine support leg part based on Abaqus finite element, and draws the impact response spectrum of the key measurement points. Through the overall response analysis of the model, the following main conclusions are drawn:

(1) The transmission of impact loads mainly starts from the base of the gas turbine, and then passes through the impact platform and the base to the legs. The stress concentration areas of the legs are mainly located at the bottom edge and the connection point with the casing. During several cycles of the impact, response peaks will occur and then rapidly decay; the local stress at the bolted connection between the leg and the casing is relatively high, which is prone to causing failure at the connection point.

(2) Under rigid installation foundation, the acceleration response of each leg of the gas turbine contains significant high-frequency components. At different positions of the same leg, the acceleration is transmitted from the bottom of the leg to the top. The amplitude of the high-frequency components shows a gradually decaying trend, while the low-frequency components become more obvious. The acceleration amplitude of the rear leg is usually higher than that of the front leg, indicating that the rear leg is subjected to greater vibration intensity and has more intense dynamic response.

(3) When the acceleration is transmitted upward from the bottom of the leg, the proportion of high-frequency component energy gradually decreases, and the total energy decays synchronously with the increase of the propagation distance. At the same time, the energy response distribution of the supporting leg has certain differences, which are related to the different energy transmission paths and the uneven distribution of structural stiffness and damping in space. These research results can provide a reference for the subsequent research on the elastic installation mode of gas turbines.

References

[1] Cheng Kaidi. Research on Transient Strong Shock Response Characteristics of Internal Supporting Bearings of Marine Gas Turbine. Harbin Engineering University, 2025. DOI:10.27060/d.cnki.ghbcu.2025.002486.

[2] Feng Linhan. Research on Global Optimization Method for Shock Resistance Performance of Ship Systems. Harbin Engineering University, 2009.

[3] Wang Jun. Research on Impact Dynamic Characteristics of Floating Shock Platform. Harbin Engineering University, 2015.

[4] Huang Shizhang, Tong Xiandong, Chen Feng, et al. Experimental Study on Shock Response of Scaled Model of Marine Gas Turbine. Shipbuilding of China, 2024, 65(6):118-129.

[5] Ding Jianjun, Zhang Zhongyu, Tian Zhaoli,

et al. Research on Dynamic Response of Ship Piping Under Underwater Explosion Shock. Ship & Boat, 2012, 23(5): 38-42.

[6] Gao Chenchen. Research on Shock Resistance Characteristics of Vibration Isolation System for Gas Turbine Simulation Device. Shenyang University of Technology, 2025. DOI:10.27322/d.cnki.gsgyu.2025.000681.

[7] Yao Xiongliang, Xiong Banghu, Wang Zhikai, et al. Transmission Characteristics of Underwater Explosion Shock Wave Load along Gas Turbine Structure. Acta Armamentarii, 2022, 43(9): 2367-2378.

[8] Liu Jianhu, Pan Jianqiang, He Bin. Comparison of Equipment Shock Resistance Standards of Major Naval Countries. Applied Science and Technology, 2010, 37(9):17-25.

[9] Xiong Banghu. Research on Transient Strong Impact Analysis Method and Response Characteristics of Marine Gas Turbine Components. Harbin Engineering University, 023.DOI:10.27060/d.cnki.ghbcu.2023.002309.

[10] Li Yanjun, Chen Xu, Zeng Qingpeng, et al. Review of anti-shock evaluation methods for ship power equipment. Chinese Journal of Ship Research, 2024, 19(3): 61-85. DOI: 10.19693/j.issn.1673-3185.03443.

[11] Sun Qikai, Zhang Nan, Liu Xiao, et al. Dynamic Reduction Coefficient of Steel-concrete Composite Beams Based on Timoshenko Beam Theory. Journal of Jilin University (Engineering and Technology Edition), 2023, 53(2): 488-495. DOI:10.13229/j.cnki.jdxbgxb.20210742.

 Copyright @ STEMM Institute Press